Hybrid Active Filter With Variable Conductance for Harmonic Resonance Suppression in Industrial Power Systems

Tzung-Lin Lee, *Member, IEEE*, Yen-Ching Wang, *Student Member, IEEE*, Jian-Cheng Li, and Josep M. Guerrero, *Senior Member, IEEE*

***Abstract*—Unintentional series and/or parallel resonances, due to the tuned passive filter and the line inductance, may result in severe harmonic distortion in the industrial power system. This paper presents a hybrid active filter to suppress harmonic resonance and to reduce harmonic distortion. The proposed hybrid filter is operated as variable harmonic conductance according to the voltage total harmonic distortion; therefore, harmonic distortion can be reduced to an acceptable level in response to load change or parameter variation of the power system. Since the hybrid filter is composed of a seventh-tuned passive filter and an active filter in series connection, both dc voltage and kVA rating of the active filter are dramatically decreased compared with the pure shunt active filter. In real application, this feature is very attractive since the active power filter with fully power electronics is very expensive. A reasonable tradeoff between filtering performances and cost is to use the hybrid active filter. Design consideration are presented, and experimental results are provided to validate effectiveness of the proposed method. Furthermore, this paper discusses filtering performances on line impedance, line resistance, voltage unbalance, and capacitive filters.**

***Index Terms*—Harmonic resonance, hybrid active filter, industrial power system.**

Nomenclature

v_s	Source voltage.
i_s	Source current.
i_L	Load current.
i	Filter current.
L_s	Source inductor.
R_s	Source resistor.
L_f	Filter inductor.
C_f	Filter capacitor.
R_f	Filter resistor.
$C_{\rm dc}$	DC capacitor of the hybrid filter.
$v_{\rm dc}$	DC voltage of the hybrid filter.
$v^*_{\rm dc}$	DC voltage command.
e	Terminal voltage.
e^e_{qd}	Terminal voltage in the synchronous reference frame (SRF).
$e^e_{qd,\,h}$	Terminal harmonic voltage in the SRF.
e_h	Terminal harmonic voltage.
ω_h	Harmonic frequency in radians.
i^*_h	Harmonic current command.
i^*_f	Fundamental current command.
i^*	Current command.
G^*	Conductance command.
k_p	Proportional gain of the tuning control.
k_i	Integral gain of the tuning control.
K_c	Proportional gain of the current controller.
THD*	Voltage total harmonic distortion (THD) command.
I_h	Filter harmonic current amplitude.
$E(s)$	Terminal voltage in the s-domain.
$I(s)$	Filter harmonic in the s-domain.
$I^*(s)$	Filter harmonic command in s-domain.

Manuscript received October 24, 2013; revised February 20, 2014 and June 16, 2014; accepted July 28, 2014. Date of publication August 12, 2014; date of current version January 7, 2015. This work was supported by the Ministry of Science and Technology of Taiwan under Grant 103-3113-E-110-002.

T.-L. Lee and Y.-C. Wang are with the Department of Electrical Engineering, National Sun Yat-Sen University, Kaohsiung 80424, Taiwan (e-mail: tllee@mail.ee.nsysu.edu.tw; d993010012@student.nsysu.edu.tw).

J.-C. Li is with ETASIS Electronics Corporation, Taipei 241, Taiwan (e-mail: f22835014@yahoo.com.tw).

J. M. Guerrero is with the Department of Energy Technology, Aalborg University, 9220 Aalborg East, Denmark (e-mail: joz@et.aau.dk).

Color versions of one or more of the figures in this paper are available online at http://ieeexplore.ieee.org.

Digital Object Identifier 10.1109/TIE.2014.2347008

I. Introduction

HARMONIC pollution is becoming increasingly serious due to extensive use of nonlinear loads, such as adjustable speed drives, uninterruptible power supply systems, battery charging system, etc. This equipment usually uses diode or thyristor rectifiers to realize power conversion because of lower component cost and less control complexity. However, the rectifiers will contribute a large amount of harmonic current flowing into the power system, and the resulting harmonic distortion may give rise to malfunction of sensitive equipment or interfering with communication systems in the vicinity of the harmonic sources. Normally, tuned passive filters are deployed at the secondary side of the distribution transformer to provide low impedance for dominant harmonic current and correct power factor for inductive loads [1], [2]. However, due to parameter variations of passive filters, unintentional series and/or parallel resonances may occur between the passive filter and line inductance. The functionality of the passive filter may deteriorate, and excessive harmonic amplification may result [3], [4]. Thus, extra calibrating work must be consumed to maintain the filtering capability.

Various active filtering approaches have been presented to address the harmonic issues in the power system [5]–[7]. The active filter intended for compensating harmonic current

0278-0046 © 2014 IEEE. Personal use is permitted, but republication/redistribution requires IEEE permission.
See http://www.ieee.org/publications_standards/publications/rights/index.html for more information.

of nonlinear loads is the most popular one, but it may not be effective for suppressing harmonic resonances [8]. Bhattacharya and Divan proposed a hybrid series active filter to isolate harmonics between the power system and the harmonic source [9]. A so-called "active inductance" hybrid filter was presented to improve the performance of the passive filter [10]. Fujita *et al.* proposed a hybrid shunt active filter with filter-current detecting method to suppress the fifth harmonic resonance between the power system and a capacitor bank [11]. A hybrid filter in series with a capacitor bank by a coupling transformer was proposed to suppress the harmonic resonance and to compensate harmonic current [12], [13]. However, this method needs extra matching transformers or tuned passive filters to guarantee filtering functionality.

Recently, a transformerless hybrid active filter was presented to compensate harmonic current and/or fundamental reactive current [14]–[19]. Design consideration of the hybrid filter for current compensation has been extensively studied. A hybrid active filter with damping conductance was proposed to suppress harmonic voltage propagation in distribution power systems [20]. Nevertheless, this method did not consider the resonance between the passive filter and the line inductance. The fixed conductance may deteriorate the damping performances. An antiresonance hybrid filter for delta-connected capacitor bank of power-factor-correction applications was presented [21]. This circuit was limited to three single-phase inverters, and the filtering performance was not considered. In addition, the hybrid active filter was proposed for the unified power quality (PQ) conditioner to address PQ issues in the power distribution system [22]. Several case studies of the hybrid active filter considering optimal voltage or current distortion were conducted in [23].

In previous work, the authors have presented a transformerless hybrid active filter to suppress harmonic resonances in the industrial power system [24], [25]. The hybrid filter is constructed by a seventh-tuned passive filter and an active filter in series connection. It operates as a variable conductance at harmonic frequencies according to the voltage THD, so that harmonic distortion can be reduced to an acceptable level in response to load change and power system variation. Since the series capacitor is responsible for sustaining the fundamental component of the grid voltage, the active filter is able to operate with a very low dc bus voltage, compared with the pure shunt active filter [14], [20]. Hence, both the rated kVA capacity and the switching ripples are reduced accordingly. Moreover, the proposed harmonic conductance is able to avoid overcurrent of the passive filter in the case of mistuning parameters. These features will benefit practical applications.

In this paper, we further present designing consideration of the hybrid filter. A prototype circuit of the hybrid filter based on 220-V/10-kVA system has been established to verify theoretic analysis, including steady-state behavior, transient response, and stability analysis. The filtering performance of the hybrid filter is discussed considering X/R ratio and magnified variations of line impedance. We also focus on filtering deterioration due to line resistance, voltage unbalance, and capacitive filters in the power system. In many cases, an active power filter is designed to compensate harmonic current produced by a specific nonlinear load, in such a way that it needs to measure the load current to be compensated [14], [26]. In this paper, the active filter is designed as a harmonic conductance to suppress both harmonic resonance and harmonic distortion by using inverter-side voltage and current measurements. Notice that it does not require current information of the nonlinear loads. Thus, this approach can be suitable in power distribution networks in which the loads may be distributed along a feeder [20]. In addition, compensating fundamental reactive power due to unbalanced load is possible, but it is outside the scope of this paper [26], [27].

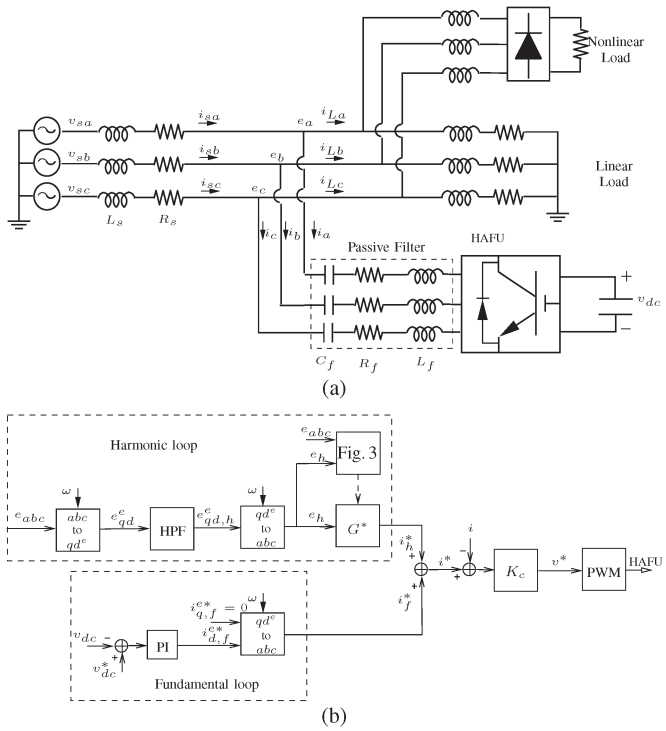

Fig. 1. Proposed HAFU in the industrial power system and its associated control. (a) Circuit diagram of the HAFU. (b) Control block diagram of the HAFU.

II. Operation Principle

Fig. 1(a) shows a simplified circuit diagram considered in this paper, where L_s represented the line inductance plus the leakage inductance of the transformer. The hybrid active filter unit (HAFU) is constructed by a seventh-tuned passive filter and a three-phase voltage source inverter in series connection. The passive filter $L_f - C_f$ is intended for compensating harmonic current and reactive power. The inverter is designed to suppress harmonic resonances and improve the filtering performances of the passive filter. Fig. 1(b) shows the overall control block diagram of the HAFU, including harmonic loop, fundamental loop, current regulator, and conductance control. A detailed principle will be presented as follows.

A. Harmonic Loop

To suppress harmonic resonances, the HAFU is proposed to operate as variable conductance at harmonic frequencies as follows:

$$i_h^* = G^* \cdot e_h \tag{1}$$

where i_h^* represents the harmonic current command. The conductance command G^* is a variable gain to provide damping for all harmonic frequencies. Harmonic voltage component e_h is obtained by using the so-called SRF transformation [9], where a phase-locked loop (PLL) is realized to determine the fundamental frequency of the power system [28]. In the SRF, the fundamental component becomes a dc value, and other harmonic components are still ac values. Therefore, harmonic voltage component $e^e_{qd,h}$ can be extracted from e^e_{qd} by using high-pass filters. After transferring back to a three-phase system, the harmonic current command i_h^* is obtained by multiplying e_h and the conductance command G^*, as shown in (1).

B. Fundamental Loop

In this paper, the q-axis is aligned to a-phase voltage. Since the passive filter is capacitive at the fundamental frequency, the passive filter draws fundamental leading current from the grid, which is located on the d-axis. The proposed inverter produces slight fundamental voltage on the d-axis, which is in phase with the fundamental leading current. Therefore, the control of dc bus voltage is able to be accomplished by exchanging real power with the grid. Thus, the current command $i^{e*}_{d,f}$ is obtained by a proportional–integral (PI) controller. The fundamental current command i_f^* in the three-phase system is generated after applying the inverse SRF transformation.

Equation (2) shows the harmonic voltage drop on the passive filter due to the compensating current of the HAFU [20], where I_h represents the maximum harmonic current of the active filter, and the voltage drop on filter resistance R_f is neglected. As can be seen, a large filter capacitor results in the reduction of the required dc voltage. On the other hand, the filter capacitor determines reactive power compensation of the passive filter at the fundamental frequency. Thus, the dc voltage $v^*_{\rm dc}$ can be determined based on this compromise. Note that the compensating current should be limited to ensure that the hybrid filter operates without undergoing saturation, i.e.,

$$v_{\rm dc} > 2\sqrt{2}\sum_h \left|\frac{1}{j\omega_h C_f} + j\omega_h L_f\right| \cdot I_h. \tag{2}$$

C. Current Regulator

The current command i^* is consisted of i_h^* and i_f^*. Based on the current command i^* and the measured current i, the voltage command v^* can be derived by using a proportional controller as follows:

$$v^* = K_c \cdot (i^* - i) \tag{3}$$

where K_c is a proportional gain. According to the voltage command v^*, space-vector pulsewidth modulation (PWM) is employed to synthesize the required output voltage of the inverter. Fig. 2 shows the model of the current control. The computational delay of digital signal processing is equal to one sampling delay T, and PWM delay approximates to half sampling delay $T/2$. Hence, the proportional gain K_c can be simply evaluated from both open-loop and closed-loop gains for suitable stability margin and current tracking capability. The frequency-domain analysis of current control will be given in Section IV.

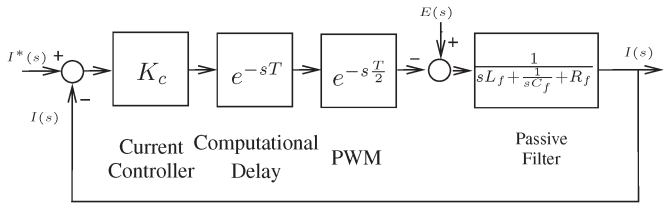

Fig. 2. Closed-loop model of the current control.

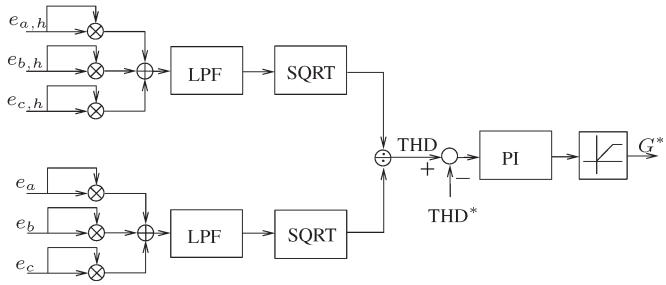

Fig. 3. Conductance control block diagram.

D. Conductance Control

Fig. 3 shows the proposed conductance control. The harmonic conductance command G^* is determined according to the voltage THD at the HAFU installation point. The voltage THD is approximately calculated by the control shown in Fig. 3. Here, two low-pass filters (LPFs) with cutoff frequency $f_{\rm LP} = 20$ Hz are realized to filter out ripple components [29], [30]. The error between the allowable THD* and the measured THD is then fed into a PI controller to obtain the harmonic conductance command G^*. The allowable distortion could be referred to the harmonic limit in IEEE std. 519-1992 [31]. Note that PI parameters need to be tuned for required response and stability. For example, the proportional gain can be tuned for transient behavior, and the integral gain is responsible for suppressing the steady-state error. The bandwidth should be lower than one-tenth of the cutoff frequency of the current loop to assure stable operation. This way, the HAFU is able to dynamically adjust G^* to maintain harmonic distortion at an allowable level.

III. Analysis of Filtering Performance

The filtering performance of the HAFU has been addressed in [25] by developing equivalent circuit models, in which both harmonic impedance and harmonic amplification are considered. The frequency characteristic of the passive filter is changed by the proposed harmonic conductance to avoid unintentional resonances. Here, we will concentrate on the damping performance with variation of line impedance L_s, line resistance R_s, and THD*. Voltage unbalance and filter capacitors in the power system are also considered.

A. L_s on Damping Performances

Fig. 4 shows voltage THD for various values of L_s. The fifth harmonic voltage is severely amplified at $L_s = 0.3$ mH (2.3%),

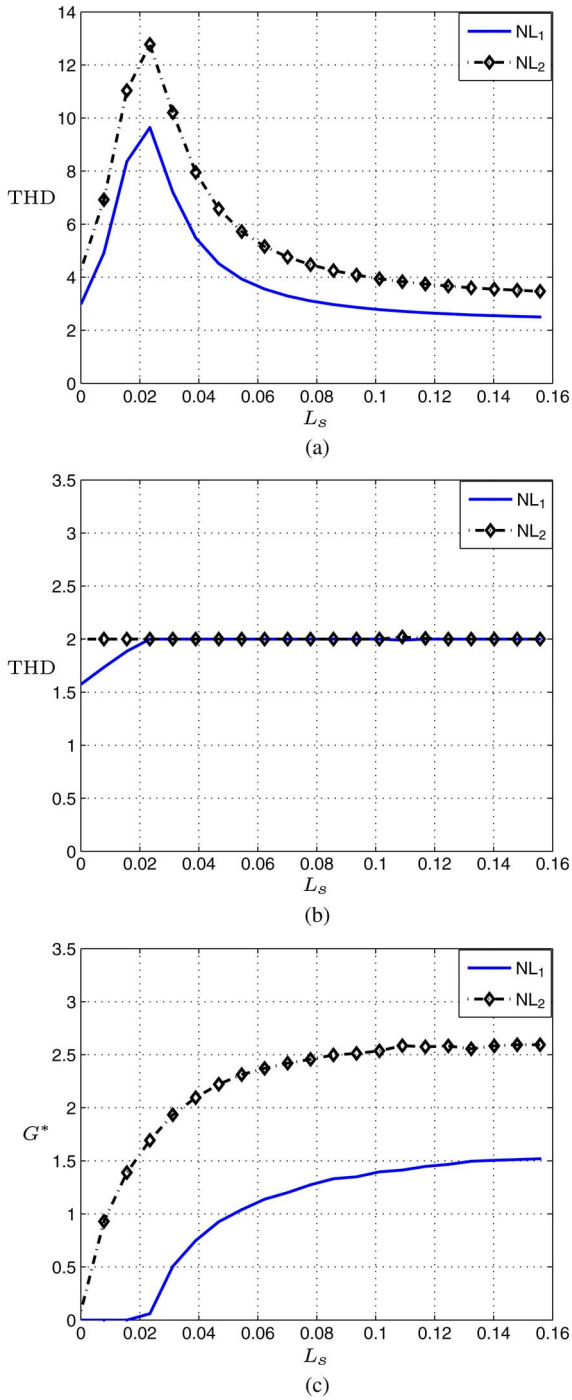

Fig. 4. Voltage THD (%) and the required G^* (p.u.) with varying line impedance L_s (p.u.). (a) Voltage THD at e when the HAFU is off. (b) Voltage THD at e when the HAFU is on. (c) G^* when the HAFU is on.

as shown in Fig. 4(a). This resonance is alleviated if L_s is not equal to 2.3%. However, voltage distortion is still significant due to harmonic voltage drop on L_s. After the HAFU is started, Fig. 4(b) shows voltage distortion is maintained at 2% by increasing G^*, as shown in Fig. 4(c). It is worth noting that the HAFU is operated at antiresonance mode, i.e., $G^* = 0$, if L_s is less than 2.3% for NL_1. This means that the voltage distortion is less than 2%. At that time, a lower THD* command is needed to further reduce the current distortion of i_s.

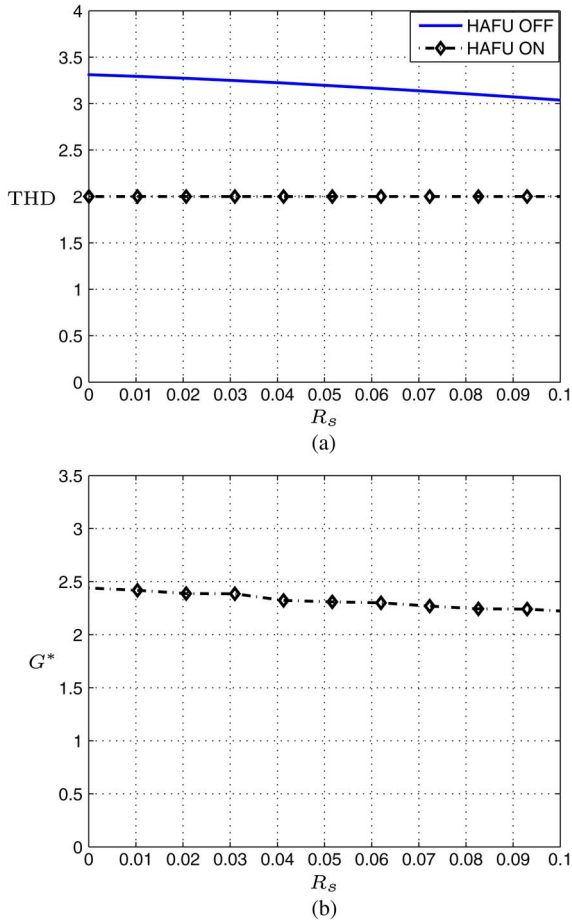

Fig. 5. Voltage THD (%) and the required G^* (p.u.) with varying line resistance R_s (p.u.). (a) Voltage THD at e. (b) G^* when the HAFU is on.

B. R_s on Damping Performances

In the low-voltage system, the X/R ratio becomes lower, and line resistance on damping performances must be taken into consideration. Fig. 5(a) shows voltage distortion with varying R_s for NL_2. Since increasing R_s could help in reducing voltage distortion, the required conductance to maintain voltage distortion at 2% is accordingly reduced, as shown in Fig. 5(b). From this observation, the HAFU could provide effective damping capability, although R_s is as large as 10%.

C. Determination of THD*

According to IEEE std. 519-1992 [31], voltage THD is limited to 5%, and individual distortion should be below 4%. Thus, THD* is set in the range of 3% and 5%. If $v_{s,h}$ and R_s are neglected, voltage THD at E, due to harmonic current load I_h, can be expressed as follows:

$$\mathrm{THD} = X_{\mathrm{pu}} \sqrt{\sum_h (h \cdot I_{h,\mathrm{pu}})^2}. \tag{4}$$

X represents the series impedance of both L_s and leakage inductance of transformer. Here, we will consider three cases in Table I to illustrate how to determine voltage THD*, where only the fifth and seventh harmonics are considered. In the

TABLE I
CALCULATION OF THD*

	$I_{5,pu}$	$I_{7,pu}$	THD
Case 1	0.04	0.03	$0.2X_{pu}$
Case 2	0.035	0.035	$0.22X_{pu}$
Case 3	0.03	0.04	$0.32X_{pu}$

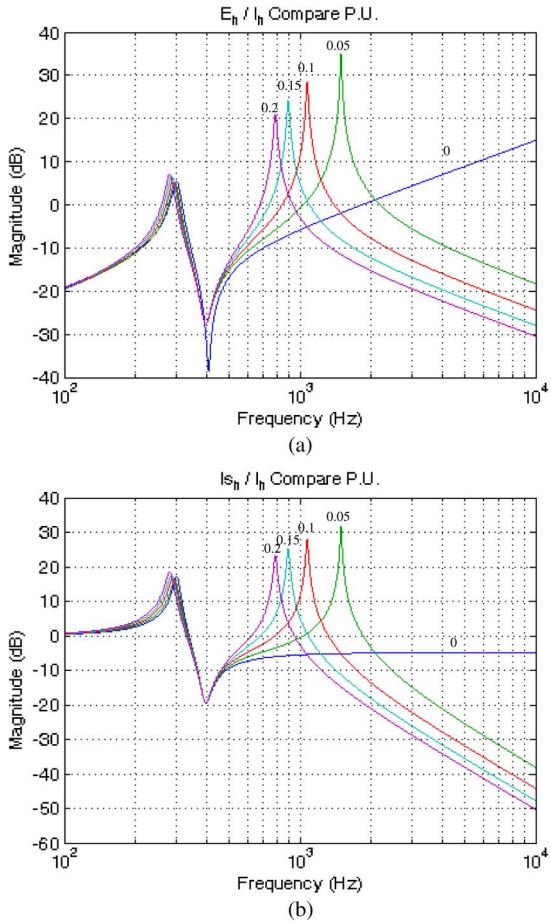

Fig. 6. Harmonic amplification considering different passive filter capacitors C_e (0.05, 0.1, 0.15, and 0.2 p.u.). (a) Harmonic impedance. (b) Source current amplification.

first one, the fifth harmonic is dominant; therefore, THD* lower than $0.2X_{\rm pu}$ is a sufficient condition to confirm with the harmonic limit. If the fifth and seventh harmonics have the same distortion, THD* $= 0.22X_{\rm pu}$ is acceptable. When the seventh harmonic becomes critical, THD* $= 0.32X_{\rm pu}$ works in the third case. Therefore, the first case is the critical one to determine the required THD*. Note that THD* should be reduced to enhance filtering capability in the case of low system impedance.

D. Capacitive Filters

In power electronic equipment, LPFs or electromagnetic interference (EMI) filters are usually installed at the grid side of the inverter to alleviate switching ripples into the power system. Since these filters present capacitive characteristics, harmonic resonances may unintentionally occur [32]–[36]. This scenario becomes much more significant in the so-called microgrid system because a large number of output filters installed

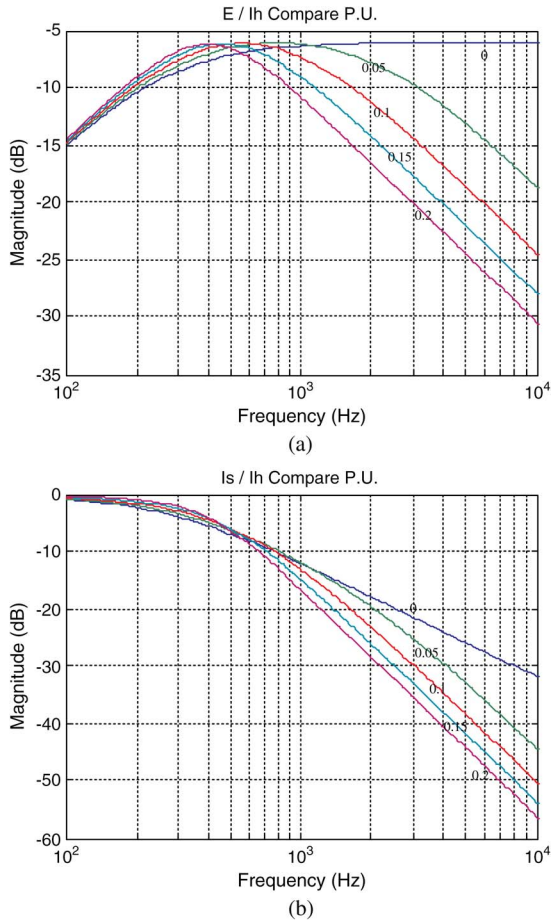

Fig. 7. Damping performances for different passive filter capacitors C_e (0.05, 0.1, 0.15, and 0.2 p.u.) with $G^* = 2.0$ p.u. (a) Harmonic impedance. (b) Source current amplification.

by the inverter-based distributed generators may participate in resonances [37]. Fig. 6 shows harmonic impedance and source current amplification for different capacitors C_e installed at the power capacitor chip. As can be seen, C_e shifts the resonant frequency and induce another high-frequency resonance, which may result in serious harmonics. Simulation results in Fig. 7 show that amplification of E_h and $i_{s,h}$ can be effectively suppressed by the proposed hybrid filter. Note that the filtering capability is dependent on the bandwidth of the HAFU.

E. Voltage Unbalance

The voltage unbalance in a low-voltage system is usually significant due to high line impedance and uneven distribution of single-phase loads [38]. Large unbalance may cause second-order harmonics in executing SRF control of the HAFU. In this sense, we need to add a band-rejected filter tuned at the second-order harmonic frequency in Fig. 1 to reduce this unwanted component. We also can use second-order-generalized-integrator-based methods to separate negative-sequence component [39] in the proposed control. It is worth nothing that unbalanced voltage or unbalanced current is possible to be compensated by the proposed HAFU. In this case, the HAFU has to generate fundamental negative-sequence voltage. This issue is open for further research.

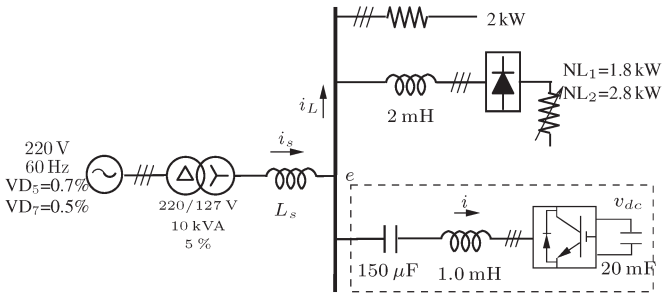

Fig. 8. Experimental setup.

TABLE II
EXPERIMENTAL PARAMETERS

Power system	220 V(L-L), 60 Hz, VD_5=0.7%, VD_7=0.5%
Transformer	220/127 V, 10 kVA, impedance 5%
Resistive load	2kW(20 %)
Nonlinear load	NL_1=1.8kW(18 %), NL_2=2.8kW(28 %)
Passive filter	$L_f = 1.0$ mH(7.8 %), $C_f = 150\ \mu$F(27 %) $Q_f = 20$
Switching frequency	10 kHz
Sampling frequency	20 kHz
Current control	k_c=5 V/A
DC voltage control	k_p=1 A/V , k_i=100 A/(V · s), v_{dc}^*=50V
Tuning control	k_p=1 A/V , k_i=500 A/(V · s), THD*=2.0% f_{HP}=10 Hz, f_{LP}=20 Hz

TABLE III
BASE VALUE

Voltage	220 V
kVA	10 kVA
Impedance	4.84 Ω
Conductance	0.207 Ω^{-1}

IV. EXPERIMENTAL VERIFICATION

A power stage setup was built and tested as shown in Fig. 8. Table II gives experimental parameters based on the per unit system in Table III. VD_5 and VD_7 represent the fifth and seventh voltage distortions in the laboratory, respectively. The filter capacitor C_F is designed to compensate inductive load, and the filter inductor L_F is chosen so that the LC filter is resonant at the seventh-order harmonic frequency. The dc link capacitor is based on the allowed voltage ripple (5%). The control of the hybrid filter was implemented by the evaluation platform of the TMS320F28335 chip [40] to perform the PLL, the synchronous reference frame transformation, LPFs, PI controllers, current regulator, A/D conversion, and PWM units. Note that the OFF state of the HAFU corresponds to turning on three upper switches and turning off three lower switches, which means the three phases of the inverter are short-circuited. At this moment the HAFU works as a pure passive filter.

A. Three-Phase Load

Figs. 9 and 10 show the grid voltage e, the source current i_s, the filter current i, and the load current i_L for $NL_1 = 1.8$ kW and $NL_2 = 2.8$ kW, respectively. When the HAFU is in the OFF state, the HAFU becomes a passive filter. Since the resonant frequency between the passive filter $L_f - C_f$ and line inductance L_s is close to the fifth harmonic frequency, fifth harmonic distortion on e, i_s, i_f are significantly amplified as

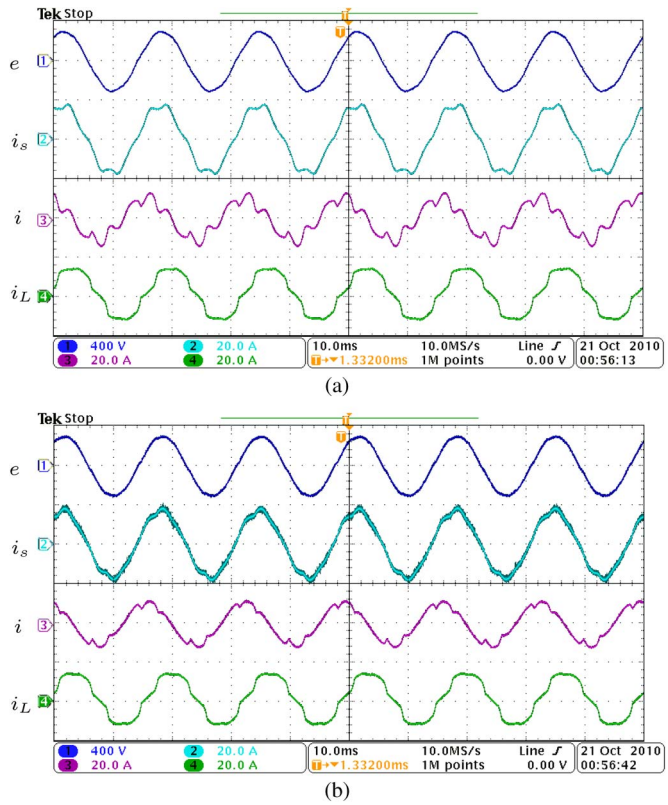

Fig. 9. Line voltage e, source current i_s, load current i_L, and filter current i in the case of NL_1 initiated. X-axis: 5 ms/div. (a) HAFU is off. (b) HAFU is on.

shown in Figs. 9(a) and 10(a). As can be seen, the passive filter loses its filtering functionality and even causes excessive harmonic current in i_s or harmonic voltage on e. It is worth noting that the resonant frequency could be shifted toward the lower frequency due to the existence of the leakage inductance of the transformer.

After the start of the HAFU, the harmonic distortion is clearly improved as shown in Figs. 9(b) and 10(b). The THD of e is reduced to 2.0% with $G^* = 0.97$ p.u. for NL_1 and $G^* = 3.05$ p.u. for NL_2, respectively. The THD of i_s is also improved below 5% in both cases. Tables IV and V summarize THD data of e, i_s, and i, i_L measured by a PQ analyzer (HIOKI 3196). High-order harmonics (>13) are not included here due to insignificance. Seventh harmonic voltage distortion is increased after the HAFU is started. This is because the HAFU emulates conductance for all harmonic frequencies. This feature can be used to avoid the overloading of the passive filter at the tuned (seventh) frequency. We also observe that fifth harmonic component of load current i_L is slightly increased. This may result from improvement of the fifth voltage distortion on e.

The detailed results indicate that the proposed HAFU is able to suppress harmonic resonances and to reduce harmonic distortion. More importantly, the HAFU only consumes 470 VA, which is approximately 4.7% of the system rating or 16.7% of NL_2. Obviously, the required kVA rating of the filter is significantly reduced, in comparison with the use of a pure shunt active power filter.

Fig. 11 shows the transient waveforms of G^*, THD of e, and v_{dc} as the nonlinear load is changed by a stepped increase from

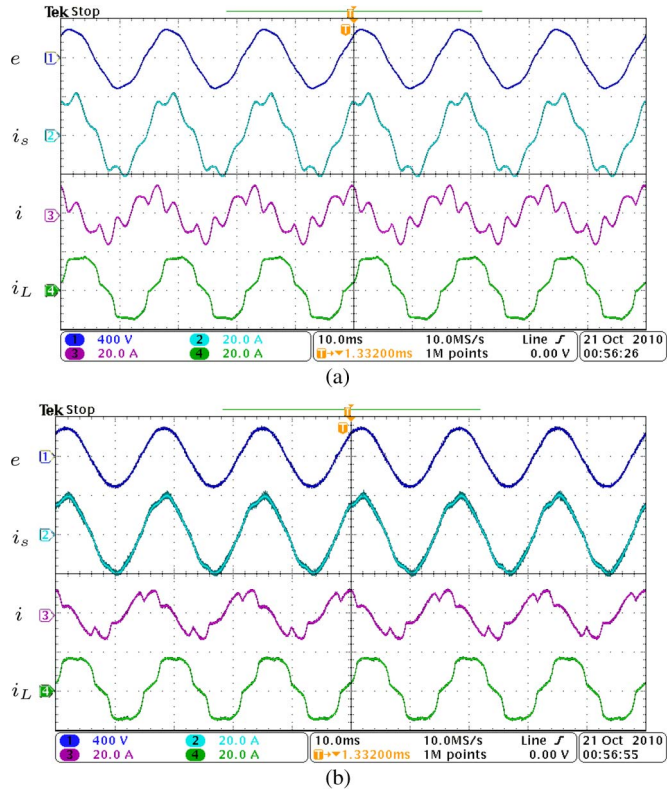

Fig. 10. Line voltage e, source current i_s, load current i_L, and filter current i in the case of NL_2 initiated. X-axis: 5 ms/div. (a) HAFU is off. (b) HAFU is on.

TABLE IV
HARMONIC DISTORTION FOR $NL_1 = 1.8$ kW. (a) VOLTAGE DISTORTION OF e. (b) CURRENT DISTORTION OF i_s. (c) CURRENT DISTORTION OF i_L. (d) CURRENT DISTORTION OF i

(a)

	THD	HD_5	HD_7	HD_{11}	HD_{13}
HAFU OFF	2.9%	2.7%	0.1%	0.5%	0.4%
HAFU ON	2.0%	1.6%	0.9%	0.5%	0.4%

(b)

	THD	HD_5	HD_7	HD_{11}	HD_{13}
HAFU OFF	8.5%	8.2%	1.7%	0.3%	0.2%
HAFU ON	4.8%	3.7%	2.8%	0.4%	0.4%

(c)

	THD	HD_5	HD_7	HD_{11}	HD_{13}
HAFU OFF	9.1%	7.3%	4.3%	2.8%	1.6%
HAFU ON	9.1%	7.7%	3.4%	2.5%	1.5%

(d)

	THD	HD_5	HD_7	HD_{11}	HD_{13}
HAFU OFF	27%	25%	9.2%	3.7%	2.3%
HAFU ON	12%	8.9%	6.7%	3.7%	2.0%

NL_1 to NL_2 at T. Large nonlinear current will result in large voltage distortion on e. Due to the proposed tuning control, the conductance command G^* is increased to 3.05 p.u. to draw more harmonic current shown in Fig. 11(b) in order to maintain voltage THD at 2%. Fig. 11(a) also demonstrates v_{dc} is well controlled to 50 V to ensure proper operation of the active filter.

B. Comparison With Current-Compensating Method

Additionally, time-domain simulations have been carried out to compare filtering performances between current-compensating and voltage-damping hybrid active filters. In the current-compensating case, the load current is measured, and harmonic components are extracted by using synchronous reference frame transformations [14], [26]. In Fig. 12, source current THDs and individual harmonic distortions are given for both light and heavy nonlinear load conditions. As shown, both methods are able to reduce source current distortion, and their filtering performances are similar. Further, by using the

TABLE V
HARMONIC DISTORTION FOR $NL_2 = 2.8$ kW. (a) VOLTAGE DISTORTION OF e. (b) CURRENT DISTORTION OF i_s. (c) CURRENT DISTORTION OF i_L. (d) CURRENT DISTORTION OF i

(a)

	THD	HD_5	HD_7	HD_{11}	HD_{13}
HAFU OFF	4.6%	4.5%	0.1%	0.6%	0.4%
HAFU ON	2.0%	1.6%	0.8%	0.5%	0.3%

(b)

	THD	HD_5	HD_7	HD_{11}	HD_{13}
HAFU OFF	17%	16%	2.1%	0.6%	0.3%
HAFU ON	4.3%	3.3%	2.1%	0.4%	0.4%

(c)

	THD	HD_5	HD_7	HD_{11}	HD_{13}
HAFU OFF	13%	10%	6.5%	3.6%	2.2%
HAFU ON	14%	13%	5.5%	3.7%	2.1%

(d)

	THD	HD_5	HD_7	HD_{11}	HD_{13}
HAFU OFF	43%	41%	13%	4.5%	2.7%
HAFU ON	21%	17%	9.2%	5.6%	3.0%

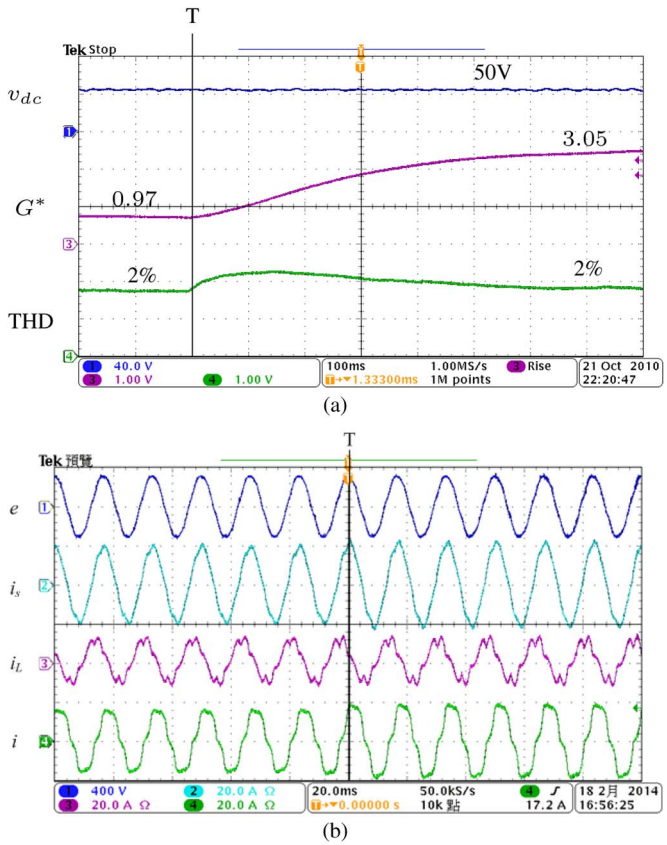

Fig. 11. Transient response when the nonlinear load is increased at T. (a) Waveforms of v_{dc}, Voltage THD, G^*. X-axis: 100 ms/div; Y-axis: v_{dc} (V), G^* (1.21 p.u./div), and THD (1.25%/div). (b) Current waveforms.

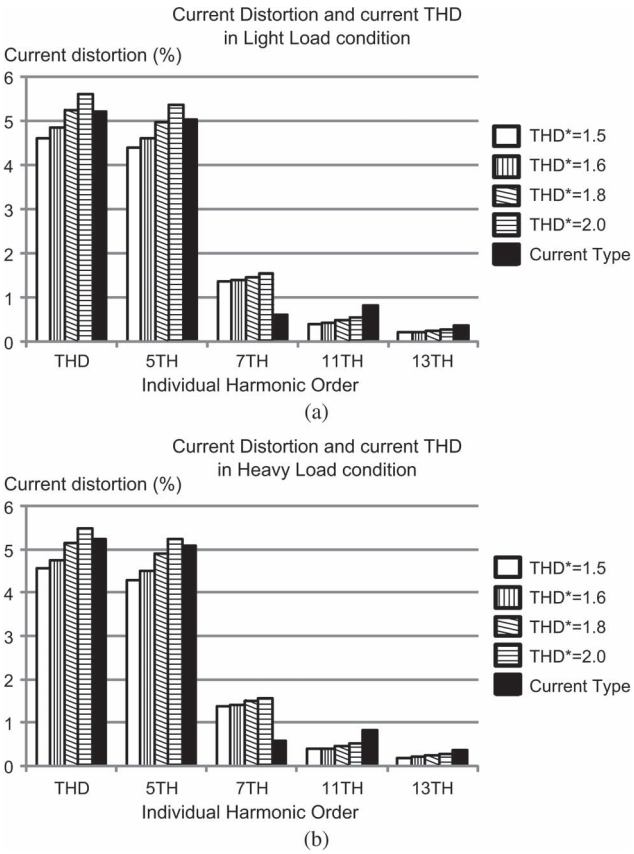

Fig. 12. Comparison of filtering performances between current-compensating and voltage-damping hybrid active filters. (a) Current distortion in light load condition. (b) Current distortion in heavy load condition.

proposed approach, a small voltage THD* value can provide even better filtering results, e.g., THD$^* < 1.8\%$. In [26], experimental results of the current-compensating hybrid active filter show that source current distortion can be reduced from 14.2% to 4.3%, which are similar to the results of the proposed voltage-damping hybrid filter given in Table V.

C. Single-Phase Load

In addition, filtering experiment considering single-phase nonlinear load is conducted. The setup of three-phase diode rectifier is changed to a single phase one by adding a smooth dc capacitor of 560 μF. Since the nonlinear load is connected between a-phase and b-phase, large third-order harmonic current is generated between them. As shown in Fig. 13, harmonic current is amplified between the source current i_s and the filter current i. After the HAFU is started, harmonic resonance is suppressed, and current distortion is reduced as indicated in Fig. 14. Test results are summarized in Table VI. Voltage distortion of e is reduced from 4.6% to 3.0% with conductance command $G^* = 0.5$ p.u. Since the passive filter is tuned at the seventh-order harmonic frequency, the proposed hybrid filter is not able to suppress third-order harmonic distortion effectively for single-phase nonlinear load. In this case, the passive filter might be tuned at fifth-order harmonic frequency to improve filtering performance for third-order harmonic.

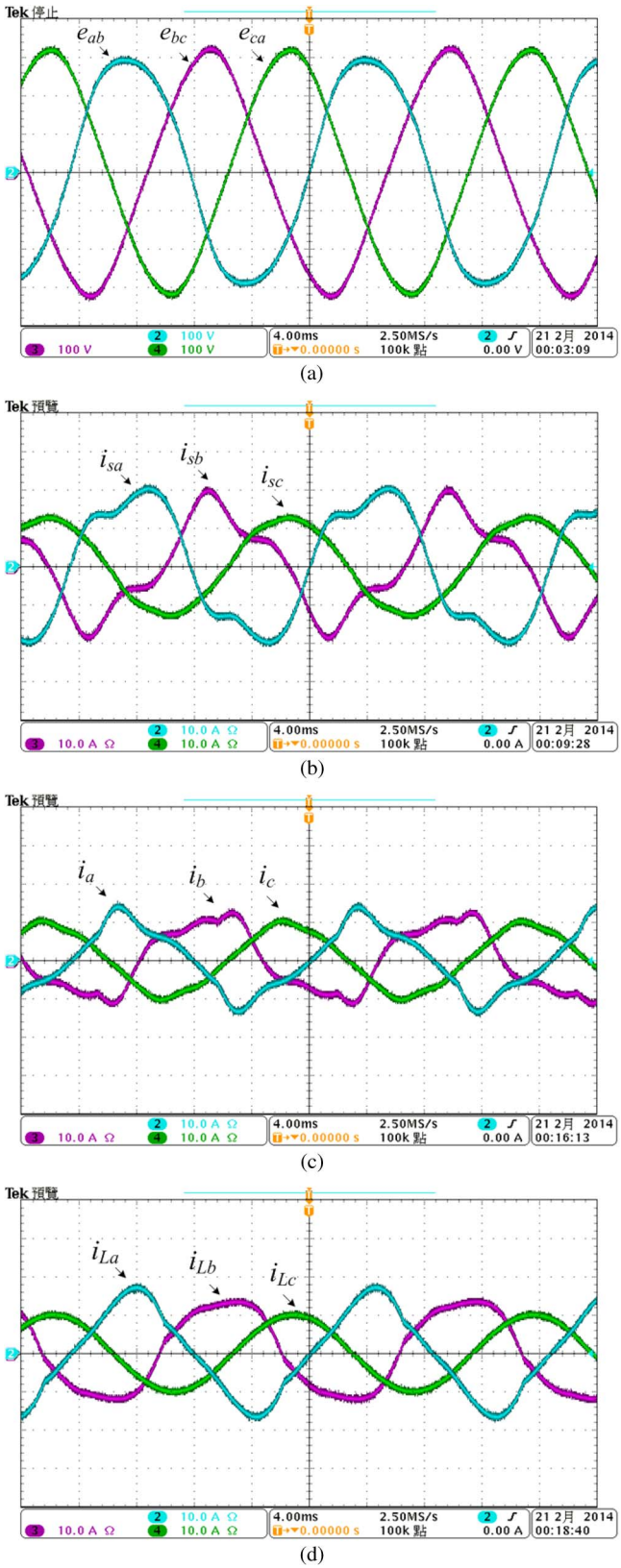

Fig. 13. HAFU is off for single-phase nonlinear load. (a) Terminal voltage. (b) Source current. (c) Filter current. (d) Load current.

D. Stability Analysis

The open-loop gain of the current control can be obtained according to Fig. 2. As shown in Fig. 15(a), the resonant

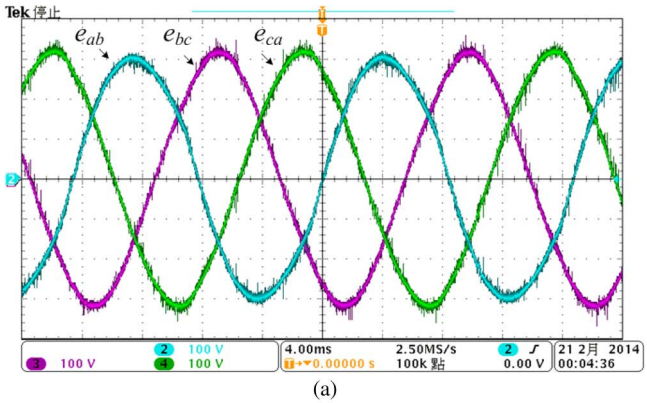

(a)

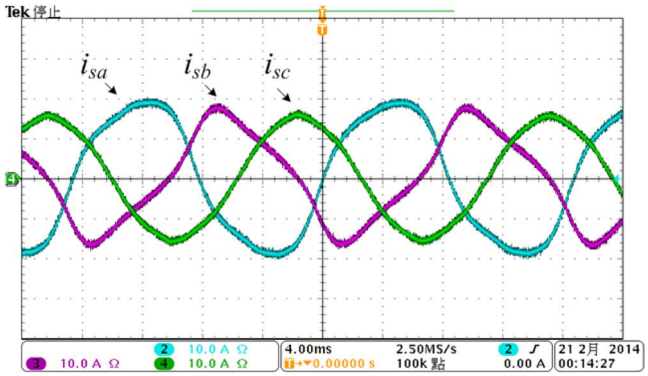

(b)

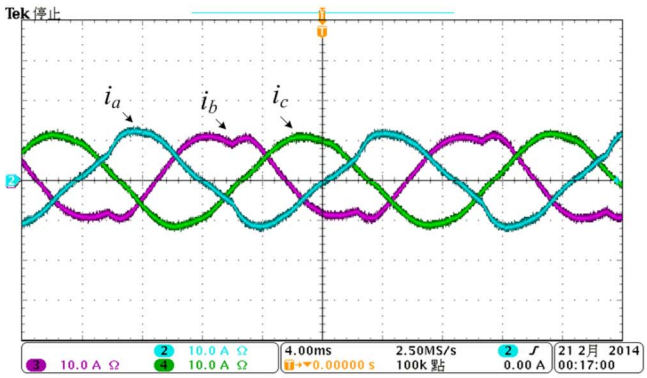

(c)

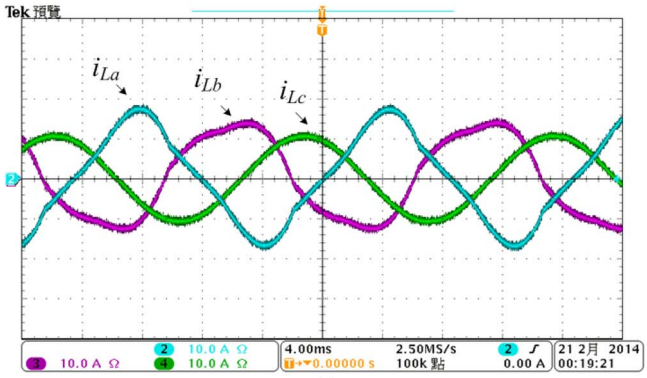

(d)

Fig. 14. HAFU is on for single-phase nonlinear load. (a) Terminal voltage. (b) Source current. (c) Filter current. (d) Load current.

peak is due to the passive filter. In this paper, the proportional gain K_c is chosen so that the bandwidth is approximately 970 Hz with a phase margin of 83°. The closed-loop gain in

TABLE VI
HARMONIC DISTORTION FOR SINGLE-PHASE NONLINEAR LOAD. (a) VOLTAGE DISTORTION OF e. (b) CURRENT DISTORTION OF i_s. (c) CURRENT DISTORTION OF i_L. (d) CURRENT DISTORTION OF i

(a)

	e_{ab}	e_{bc}	e_{ca}
HAFU OFF	6.3%	4.1%	2.4%
HAFU ON	4.1%	2.6%	1.8%

(b)

	i_{sa}	i_{sb}	i_{sc}
HAFU OFF	19%	28%	3.8%
HAFU ON	12%	16%	2.5%

(c)

	i_{La}	i_{Lb}	i_{Lc}
HAFU OFF	13%	13%	1.2%
HAFU ON	13%	13%	1.2%

(d)

	i_a	i_b	i_c
HAFU OFF	22%	25%	6.4%
HAFU ON	11%	12%	4.7%

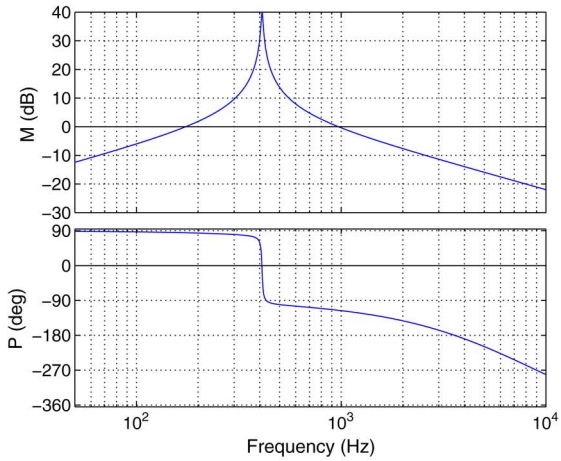

(a)

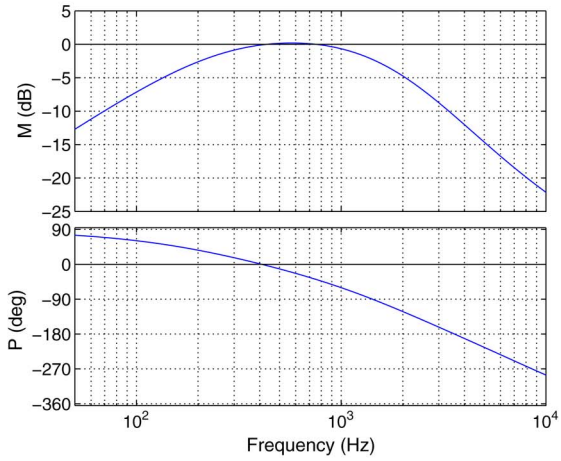

(b)

Fig. 15. Frequency domain analysis of current control. (a) Open-loop gain. (b) Closed-loop gain.

Fig. 15(b) also demonstrates that current tracking performance is acceptable for low-order harmonic frequencies. However, the current control can be further improved by using the so-called resonant controller [41], [42].

V. Conclusion

This paper presents a hybrid active filter to suppress harmonic resonances in industrial power systems. The proposed hybrid filter is composed of a seventh harmonic-tuned passive filter and an active filter in series connection at the secondary side of the distribution transformer. With the active filter part operating as variable harmonic conductance, the filtering performances of the passive filter can be significantly improved. Accordingly, the harmonic resonances can be avoided, and the harmonic distortion can be maintained inside an acceptable level in case of load changes and variations of line impedance of the power system. Experimental results verify the effectiveness of the proposed method. Extended discussions are summarized as follows.

- Large line inductance and large nonlinear load may result in severe voltage distortion. The conductance is increased to maintain distortion to an acceptable level.
- Line resistance may help reduce voltage distortion. The conductance is decreased accordingly.
- For low line impedance, THD* should be reduced to enhance filtering performances. In this situation, measuring voltage distortion becomes a challenging issue.
- High-frequency resonances resulting from capacitive filters is possible to be suppressed by the proposed method.
- In case of unbalanced voltage, a band-rejected filter is needed to filter out second-order harmonics if the SRF is realized to extract voltage harmonics.

References

[1] R. H. Simpson, "Misapplication of power capacitors in distribution systems with nonlinear loads-three case histories," *IEEE Trans. Ind. Appl.*, vol. 41, no. 1, pp. 134–143, Jan./Feb. 2005.

[2] T. Dionise and V. Lorch, "Voltage distortion on an electrical distribution system," *IEEE Ind. Appl. Mag.*, vol. 16, no. 2, pp. 48–55, Mar./Apr. 2010.

[3] E. J. Currence, J. E. Plizga, and H. N. Nelson, "Harmonic resonance at a medium-sized industrial plant," *IEEE Trans. Ind. Appl.*, vol. 31, no. 4, pp. 682–690, Jul/Aug. 1995.

[4] C.-J. Wu *et al.*, "Investigation and mitigation of harmonic amplification problems caused by single-tuned filters," *IEEE Trans. Power Del.*, vol. 13, no. 3, pp. 800–806, Jul. 1998.

[5] B. Singh, K. Al-Haddad, and A. Chandra, "A review of active filters for power quality improvement," *IEEE Trans. Ind. Electron.*, vol. 46, no. 5, pp. 960–971, Oct. 1999.

[6] H. Akagi, "Active harmonic filters," *Proc. IEEE*, vol. 93, no. 12, pp. 2128–2141, Dec. 2005.

[7] A. Bhattacharya, C. Chakraborty, and S. Bhattacharya, "Shunt compensation," *IEEE Ind. Electron. Mag.*, vol. 3, no. 3, pp. 38–49, Sep. 2009.

[8] F. Z. Peng, "Application issues of active power filters," *IEEE Ind. Appl. Mag.*, vol. 4, no. 5, pp. 21–30, Sep./Oct. 2001.

[9] S. Bhattacharya and D. Divan, "Design and implementation of a hybrid series active filter system," in *Proc. 26th IEEE PESC*, 1995, pp. 189–195.

[10] S. Bhattacharya, P.-T. Cheng, and D. Divan, "Hybrid solutions for improving passive filter performance in high power applications," *IEEE Trans. Ind. Appl.*, vol. 33, no. 3, pp. 732–747, May/Jun. 1997.

[11] H. Fujita, T. Yamasaki, and H. Akagi, "A hybrid active filter for damping of harmonic resonance in industrial power systems," *IEEE Trans. Power Electron.*, vol. 15, no. 2, pp. 215–222, Mar. 2000.

[12] D. Detjen, J. Jacobs, R. W. De Doncker, and H.-G. Mall, "A new hybrid filter to dampen resonances and compensation harmonic currents in industrial power systems with power factor correction equipment," *IEEE Trans. Power Electron.*, vol. 16, no. 6, pp. 821–827, Nov. 2001.

[13] V. Verma and B. Singh, "Design and implementation of a current-controlled parallel hybrid power filter," *IEEE Trans. Ind. Appl.*, vol. 45, no. 5, pp. 1910–1917, Sep./Oct. 2009.

[14] H. Akagi, S. Srianthumrong, and Y. Tamai, "Comparison in circuit configuration and filtering performance between hybrid and pure shunt active filters," in *Conf. Rec. 38th IEEE IAS Annu. Meeting*, 2003, pp. 1195–1202.

[15] C.-S. Lam, W.-H. Choi, M.-C. Wong, and Y.-D. Han, "Adaptive DC-link voltage-controlled hybrid active power filters for reactive power compensation," *IEEE Trans. Power Electron.*, vol. 27, no. 4, pp. 1758–1772, Apr. 2012.

[16] A. Bhattacharya, C. Chakraborty, and S. Bhattacharya, "Parallel-connected shunt hybrid active power filters operating at different switching frequencies for improved performance," *IEEE Trans. Ind. Electron.*, vol. 59, no. 11, pp. 4007–4019, Nov. 2012.

[17] S. Rahmani, K. Hamadi, and A. Al-Haddad, "A Lyapunov-function-based control for a three-phase shunt hybrid active filter," *IEEE Trans. Ind. Electron.*, vol. 59, no. 3, pp. 1418–1429, Mar. 2012.

[18] S. Rahmani, A. Hamadi, K. Al-Haddad, and L. Dessaint, "A combination of shunt hybrid power filter and thyristor-controlled reactor for power quality," *IEEE Trans. Ind. Electron.*, vol. 61, no. 5, pp. 2152–2164, May 2014.

[19] C.-S. Lam *et al.*, "Design and performance of an adaptive low-DC-voltage-controlled LC-hybrid active power filter with a neutral inductor in three-phase four-wire power systems," *IEEE Trans. Ind. Electron.*, vol. 61, no. 6, pp. 2635–2647, Jun. 2014.

[20] R. Inzunza and H. Akagi, "A 6.6-kV transformerless shunt hybrid active filter for installation on a power distribution system," *IEEE Trans. Power Electron.*, vol. 20, no. 4, pp. 893–900, Jul. 2005.

[21] P. Jintakosonwit, S. Srianthumrong, and P. Jintagosonwit, "Implementation and performance of an anti-resonance hybrid delta-connected capacitor bank for power factor correction," *IEEE Trans. Power Electron.*, vol. 22, no. 6, pp. 2543–2551, Nov. 2007.

[22] K. Karanki, G. Geddada, M. Mishra, and B. Kumar, "A modified three-phase four-wire UPQC topology with reduced DC-link voltage rating," *IEEE Trans. Ind. Electron.*, vol. 60, no. 9, pp. 3555–3566, Sep. 2013.

[23] A. Zobaa, "Optimal multiobjective design of hybrid active power filters considering a distorted environment," *IEEE Trans. Ind. Electron.*, vol. 61, no. 1, pp. 107–114, Jan. 2014.

[24] T.-L. Lee, Y.-C. Wang, and J.-C. Li, "Design of a hybrid active filter for harmonics suppression in industrial facilities," in *Proc. IEEE PEDS*, 2009, pp. 121–126.

[25] T.-L. Lee, Y.-C. Wang, and J. Guerrero, "Resonant current regulation for transformerless hybrid active filter to suppress harmonic resonances in industrial power systems," in *Proc. IEEE APEC Expo.*, 2010, pp. 380–386.

[26] Y.-C. Wang and T.-L. Lee, "A control strategy of hybrid active filter to compensate unbalanced load in three-phase three-wire power system," in *Proc. IEEE PEDG Syst.*, 2012, pp. 450–456.

[27] T.-L. Lee, S.-H. Hu, and Y.-H. Chan, "D-STATCOM with positive-sequence admittance and negative-sequence conductance to mitigate voltage fluctuations in high-level penetration of distributed-generation systems," *IEEE Trans. Ind. Electron.*, vol. 60, no. 4, pp. 1417–1428, Apr. 2013.

[28] V. Kaura and V. Blasko, "Operation of a phase locked loop system under distorted utility conditions," *IEEE Trans. Ind. Appl.*, vol. 33, no. 1, pp. 58–63, Jan./Feb. 1997.

[29] P. Jintakosonwit, H. Akagi, H. Fujita, and S. Ogasawara, "Implementation and performance of automatic gain adjustment in a shunt active filter for harmonic damping throughout a power distribution system," *IEEE Trans. Power Electron.*, vol. 17, no. 3, pp. 438–447, Mar. 2002.

[30] P. Jintakosonwit, H. Fujita, H. Akagi, and S. Ogasawara, "Implementation and performance of cooperative control of shunt active filters for harmonic damping throughout a power distribution system," *IEEE Trans. Ind. Appl.*, vol. 39, no. 2, pp. 556–564, Mar./Apr. 2003.

[31] *IEEE Recommended Practices and Requirements for Harmonic Control in Electrical Power Systems*, IEEE Std. 519-1992, 1993.

[32] V. Blasko and V. Kaura, "A novel control to actively damp resonance in input LC filter of a three-phase voltage source converter," *IEEE Trans. Ind. Appl.*, vol. 33, no. 2, pp. 542–550, Mar./Apr. 1997.

[33] P. C. Loh and D. G. Holmes, "Analysis of multiloop control strategies for LC/CL/LCL-filtered voltage-source and current-source inverters," *IEEE Trans. Ind. Appl.*, vol. 41, no. 2, pp. 644–654, Mar./Apr. 2005.

[34] M. Liserre, F. Blaabjerg, and S. Hansen, "Design and control of an LCL-filter-based three-phase active rectifier," *IEEE Trans. Ind. Appl.*, vol. 41, no. 5, pp. 1281–1291, Sep./Oct. 2005.

[35] E. Wu and P. W. Lehn, "Digital current control of a voltage source converter with active damping of LCL resonance," *IEEE Trans. Power Electron.*, vol. 21, no. 5, pp. 1364–1373, Sep. 2006.

[36] Y. W. Li, "Control and resonance damping of voltage-source and current-source converters with LC filters," *IEEE Trans. Ind. Electron.*, vol. 56, no. 5, pp. 1511–1521, May 2009.

[37] J. H. R. Enslin and P. J. M. Heskes, "Harmonic interaction between a large number of distributed power inverters and the distribution network," *IEEE Trans. Power Electron.*, vol. 19, no. 6, pp. 1586–1593, Nov. 2004.
[38] A. V. Jouanne and B. Banerjee, "Assessment of voltage unbalance," *IEEE Trans. Power Del.*, vol. 16, no. 4, pp. 782–790, Oct. 2001.
[39] P. Rodriguez *et al.*, "Multiresonant frequency-locked loop for grid synchronization of power converters under distorted grid conditions," *IEEE Trans. Ind. Electron.*, vol. 58, no. 1, pp. 127–138, Jan. 2011.
[40] Website of Texas Instruments 2010. [Online]. Available: http://www.ti.com/
[41] D. N. Zmood, D. G. Holmes, and G. H. Bode, "Frequency-domain analysis of three-phase linear current regulators," *IEEE Trans. Ind. Appl.*, vol. 37, no. 2, pp. 601–610, Mar./Apr. 2001.
[42] M. Castilla, J. Miret, J. Matas, L. G. De Vicuna, and J. M. Guerrero, "Linear current control scheme with series resonant harmonic compensator for single-phase grid-connected photovoltaic inverters," *IEEE Trans. Ind. Electron.*, vol. 55, no. 7, pp. 2724–2733, Jul. 2008.

Tzung-Lin Lee (S'04–M'08) received the B.S. degree from Chung Yuan Christian University, Taoyuan, Taiwan, in 1993, the M.S. degree from National Chung Cheng University, Chiayi, Taiwan, in 1995, and the Ph.D. degree from National Tsing Hua University, Hsinchu, Taiwan, in 2007, all in electrical engineering.

From 1997 to 2001, he was with the Microwave Department, Electronics Research and Service Organization, Industrial Technology Research Institute, Hsinchu, Taiwan. In September 2007, he began his teaching career at Chang Gung University, Taoyuan. Since August 2008, he has been with the Department of Electrical Engineering, National Sun Yat-Sen University, Kaohsiung, Taiwan, where he is currently an Associate Professor. His research interests include utility applications of power electronics, such as active power filters and microgrids.

Yen-Ching Wang (S'12) received the B.S. and M.S. degrees in electrical engineering from National Sun Yat-Sen University, Kaohsiung, Taiwan, in 2008 and 2010, respectively. He is currently working toward the Ph.D. degree at National Sun Yat-Sen University.

His research interests include active power filtering.

Jian-Cheng Li received the B.S. degree in electrical engineering from National Chin-Yi University of Technology, Taichung, Taiwan, in 2007 and the M.S. degree in electrical engineering from Chang Gung University, Taoyuan, Taiwan, in 2009.

He is currently a Research Engineer with ETASIS Electronics Corporation, New Taipei City, Taiwan. His current research interests include the design of switching power supplies.

Josep M. Guerrero (S'01–M'04–SM'08) received the B.S. degree in telecommunications engineering, the M.S. degree in electronics engineering, and the Ph.D. degree from the Polytechnic University of Catalonia (BarcelonaTech), Spain, in 1997, 2000, and 2003, respectively.

Since 2011, he has been a Full Professor with the Department of Energy Technology, Aalborg University, Aalborg East, Denmark, where he is responsible for the Microgrid Research Program. He is also a Guest Professor with the Chinese Academy of Sciences, Beijing, China, and Nanjing University of Aeronautics and Astronautics, Nanjing, China, and a Chair Professor with Shandong University, Jinan, China. His research interests include different microgrid aspects, including power electronics, energy storage, hierarchical and cooperative control, energy management of microgrids, and islanded minigrids.

Dr. Guerrero is an Associate Editor for the IEEE TRANSACTIONS ON POWER ELECTRONICS, the IEEE TRANSACTIONS ON INDUSTRIAL ELECTRONICS, and the *IEEE Industrial Electronics Magazine*, and an Editor for the IEEE TRANSACTIONS ON SMART GRID. In 2014, he was cited as an ISI Highly Cited Researcher.